Int. J. Electrochem. Sci., 7 **(2012)** 10074 - 10093

International Journal of
ELECTROCHEMICAL
SCIENCE
www.electrochemsci.org

Synthesis, Spectral, Thermal Analyses and Molecular Modeling of Bioactive Cu(II)-complexes with 1,3,4-thiadiazole Schiff Base Derivatives. Their Catalytic Effect on the Cathodic Reduction of Oxygen

Abdalla M. Khedr[1,*], *Hadi M. Marwani*[2,*]

[1] Chemistry Department, Faculty of Science, Tanta University, Tanta, Egypt
[2] Department of Chemistry, King Abdulaziz University, Jeddah, Saudi Arabia
[2] Center of Excellence for Advanced Materials Research, King Abdulaziz University, Jeddah, Saudi Arabia
[*] E-mails: abkhedr2001@yahoo.com (A.M. Khedr), hmarwani@kau.edu.sa (H.M. Marwani)

Received: 16 August 2012 / *Accepted:* 11 September 2012 / *Published:* 1 October 2012

New mono- and binuclear copper(II) complexes with Schiff bases derived from the condensation of 2-amino-5-substituted-aryl-1,3,4-thiadiazole with substituted aryl aldehydes were synthesized. The complexes were characterized by elemental analyses, molar conductivity, magnetic moment, IR, ^{1}H NMR, electronic, ESR and mass spectrometry as well as thermal analyses. The conductivity data of the complexes confirmed their non-electrolytic nature. An octahedral geometry was suggested for complex **1**, square-planar geometry proposed for complex **2** and square pyramidal structure suggested for complexes **3**-**7**. The 3D molecular modeling of a representative complex was carried out on a CS Chem 3-D Ultra Molecular Modeling and Analysis Program. The synthesized complexes and ligands were screened *in-vitro* for their antimicrobial activity against gram-positive bacteria (*Staphylococcus aureus*), gram-negative bacteria (*Escherichia coli*) and fungi (*Aspergillus flavus* and *Candida albicans*). In most cases, metallation increased the antimicrobial activity compared with the free ligands. Also, the catalytic effect of the prepared complexes on the cathodic reduction of oxygen was studied.

Keywords: Copper(II) complexes; thiadiazole Schiff bases; 3D molecular modeling; antimicrobial and catalytic activities

1. INTRODUCTION

The compounds containing azomethine group (-CH=N-) are known as Schiff bases. They are used as substrates in the preparation of number of industrial and biologically active compounds *via* ring closure, cyclo-addition and replacement reactions [1]. Schiff base ligands are potentially capable

of forming stable complexes with most transition metal ions, which served as model compounds for biologically important species. Schiff bases can also accommodate different metal centers involving various coordination modes thereby allowing successful synthesis of homo and hetero metallic complexes with varied stereochemistry [2]. Schiff base complexes derived from heterocyclic molecules having five membered 1,3,4-thiadiazole ring possess various pharmacological properties including analgesic [3], antimicrobial [4-6], anti-inflammatory [7], antitubercular [8], anticonvulsant [9], anticancer [10], anthelmintic [11], antiplatelet [12] and diuretic activity [13]. 2-Amino-1,3,4-thiadiazole derivatives are also used as antitumor and antituberculosis drugs [14]. Taking into consideration the above facts, seven Cu(II) complexes of Schiff bases derived from condensation of 2-amino-5-substituted-aryl-1,3,4-thiadiazole with substituted aryl aldehydes were synthesized. The complexes were characterized and evaluated for their antimicrobial activities against gram-positive (*Staphylococcus aureus*), gram-negative (*Escherichia coli*) bacteria and fungal strains (*Aspergillus flavus* and *Candida albicans*). The reactivity of these complexes towards catalytic oxygen reduction was investigated.

2. EXPERIMENTAL

2.1. Material and methods

All reagents were analytical grade products (Aldrich, Sigma or Merck) and used without further purification. Chemical analysis of carbon, nitrogen and hydrogen was performed using a Perkin–Elmer 2400 elemental analyzer. The percentage ratio of copper ions in the solid complexes was determined volumetrically using EDTA titration and thiosulfate methods [15]. Molar conductance was measured in DMF using a conductance bridge of the type 523 conductometer calibrated with KCl solution. Electron spray ionization (ESI) mass spectra were performed using a Shimadzu LCMS–2010 eV spectrometer. IR spectra of the ligand and complexes were recorded using KBr pellets in the 4000–200 cm^{-1} range on a Perkin–Elmer IR spectrophotometer model 1430. ^{1}H NMR spectra were measured at room temperature on a Bruker Avance AV-600 MHz spectrometer using the TMS as internal standard. The chemical resonances (δ) were reported in parts per million (ppm) with the ^{1}H NMR shifts referenced to the residual proton signal of deutrated solvent (DMSO-d_6). UV-Vis spectral measurements were carried out in DMSO within the wavelength range of 190-700 nm using a Shimadzu UV-Vis 240 spectrophotometer. Magnetic susceptibilities of the complexes were determined by Gouy's method using magnetic susceptibility instrument (20 Kilo Gauss). The diamagnetic corrections of the complexes were computed using Pascal's constants [16]. X-band ESR spectra of the complexes were measured on a Jeol spectrometer model JES-FE2XG using powdered samples at room temperature. Differential thermal analysis (DTA) and thermogravimetric analysis (TGA) measurements of complexes were recorded on a Shimadzu DT-50 and TG-50 thermal analyzers with heating rate of 10 °C/min from ambient temperature up to 800^{o}C. Oxford rotating disc system with speed range 0 to 3.000 rpm was used for studying the catalytic activities of the investigated Cu(II) complexes towards cathodic reduction of oxygen at a glassy carbon electrode.

2.2. Synthesis of Schiff bases

The Schiff bases were prepared by the stoichiometric reaction of 2-amino-5-substituted-aryl-1,3,4-thiadiazole with the appropriate aldehydes in a molar ratio of 1:1 (amine: aldehyde). A mixture of 0.01 mol of 2-amino-5-substituted-aryl-1,3,4-thiadiazole in ethanol, 0.01 mol of the appropriate aldehydes and 2 drops of concentrated sulphuric acid was refluxed in water bath for 5 h. The progress of the reaction was monitored at time intervals of 30 min by thin layer chromatography (TLC). When the reaction was complete the volume of alcohol was reduced to its half using a rotary evaporator. The product was poured in ice cold water to precipitate the Schiff base and then filtered off. The resulting solid was recrystallized from hot ethanol. The structures of synthesized ligands L^1–L^6 were established through the elemental analysis and spectroscopic data (IR, ^{1}H NMR and UV-Vis).

2.3. Synthesis of complexes

The Cu(II) complexes **1**-**6** were prepared by the stoichiometric reaction of the metal(II) salt with the Schiff base ligands in a molar ratio (M: L) of 1:1 whereas the Cu(II) complex **7** was prepared in a molar ratio of 2:1 (M: L). Hot ethanolic solution of the appropriate ligand (0.01 mol) and ethanolic solution of hydrated cupric sulfate (249 mg, 0.01 mol or 498 mg 0.02 mol) were mixed together with constant stirring. The mixture was refluxed for 6 h at 70–80 ºC on water bath. On cooling, the colored solid metal complexes were obtained. They were filtered off and washed several times with hot water and then with ether to remove the excess of ligand and $CuSO_4$. The solid products were dried in *vacuo* over anhydrous calcium chloride. The complexes were subjected to different spectroscopic and analytical techniques in order to deduce the composition and identity of the assembled compounds.

2.4. Molecular modeling studies

Molecular modeling of a representative complex **2** was carried out using CS Chem 3-D Ultra Molecular Modeling and Analysis Program [17-21]. For convenience of looking over the different bond lengths and bond angles, the various atoms in the compound in question are numbered in Arabic numerals.

2.5. Biological screening

The bacterial sub-cultures *Staphylococcus aureus* and *Escherichia coli* were used for anit-bacterial test whereas *Aspergillus flavus* and *Candida albicans* were used for antifungal test at the Micro-analytical unit of Cairo University using the modified Kirby–Bauer disc diffusion method [22]. Briefly, 100 mL of the tested bacteria/fungi were grown in 10 mL of fresh media until they reached 108 cells mL^{-1} for bacteria and 105 cells mL^{-1} for fungi [23]. Hundred microliters of microbial suspension was spread onto agar plates corresponding to the broth in which they were maintained. Isolated colonies of each microorganism was selected from primary agar plates and tested for

susceptibility by the disc diffusion method [24]. From the many media available, National Committee for Clinical Laboratory Standards (NCCLS) recommends Mueller–Hinton agar since it results in good batch-to-batch reproducibility. The disc diffusion method for filamentous fungi was tested using the approved standard method (M38-A), which was developed by the NCCLS [25] for evaluating the susceptibilities of filamentous fungi to antifungal agents. The disc diffusion method for yeasts was developed using the approved standard method (M44-P) by the NCCLS [26]. Plates were inoculated with filamentous fungi, *A. flavus*, at 25ºC for 48 h; Gram (+) bacteria, *S. aureus,* and Gram (-) bacteria, *E. coli*. They were incubated at 35–37ºC for 24–48 h and the yeast as *C. albicans* was incubated at 30ºC for 24–48 h. The diameters of the inhibition zones were measured in millimeters [27]. Standard discs of tetracycline (antibacterial agent) and amphotericin B (antifungal agent) served as positive controls for antimicrobial activity. However, the filter discs impregnated with 10 µL of solvent (distilled water, DMSO) were used as a negative control. The used agar (Meuller–Hinton) was rigorously tested for composition and pH. Further, the depth of the agar in the plate is a factor to be considered in the disc diffusion method. This method is well-documented and the standard zones of inhibition have been determined for susceptible and resistant values. Blank paper discs (Schleicher & Schuell, Spain) with a diameter of 8.0 mm were impregnated with 10 µL of tested concentration of the stock solutions. When a filter paper disc impregnated with a tested chemical was placed on the agar, the chemical will diffuse from the disc into the agar. This diffusion will place the chemical in the agar only around the disc. The solubility of the chemical and its molecular size will determine the area of chemical infiltration around the disc. When an organism is placed on the agar it will not grow in the area around the disc if it is susceptible to the chemical. This area of no growth around the disc is known as ‘‘zone of inhibition’’ or ‘‘clear zone’’. For the disc diffusion, the zone diameters were measured with slipping calipers of the National Committee for Clinical Laboratory Standards [27]. Agar-based methods such as Etest and disc diffusion cosidered good alternatives because they are simple and faster than broth-based methods [28, 29].

3. RESULTS AND DISCUSSION

Table 1. Physical characteristics and elemental analysis of the prepared Schiff base ligands (L^1—L^6)

Schiff base	Empirical formula (Molecular Wt.)	Color (m. p. ^oC)	Microanalysis % calc. (found)		
			%C	%H	%N
L^1	$C_{15}H_{10}N_4SO_2$ (310.33)	White (172)	58.06 (57.66)	3.25 (2.97)	18.05 (17.82)
L^2	$C_{15}H_{11}N_3SO_2$ (297.33)	Orange (168)	60.58 (60.44)	3.73 (3.97)	14.13 (13.98)
L^3	$C_{14}H_9ClN_4S$ (300.77)	Faint yellow (152)	55.91 (56.32)	3.02 (3.44)	18.63 (18.89)
L^4	$C_{15}H_9ClN_4SO_2$ (344.78)	Yellow (176)	52.26 (52.43)	2.63 (2.48)	16.25 (16.76)
L^5	$C_{16}H_{13}N_3SO_2$ (311.36)	Orange (170)	61.72 (61.92)	4.21 (4.07)	13.50 (13.87)
L^6	$C_{16}H_{15}N_5S$ (309.39)	Faint yellow (181)	62.12 (61.92)	4.89 (4.67)	22.64 (22.82)

The yield for the prepared 1,3,4-thiadiazole Schiff base was 78-83%.

The Schiff base ligands were synthesized according to scheme 1. Their purities were checked on TLC plates and the spots were visualized under ultraviolet light and by spraying with iodine vapour. The structures of all the synthesized ligands (L^1-L^6) were established through the elemental analyses (Table 1), IR, ^{1}H NMR and UV-Vis spectral data. These ligands were used for the preparation of Cu(II) complexes (1-7).

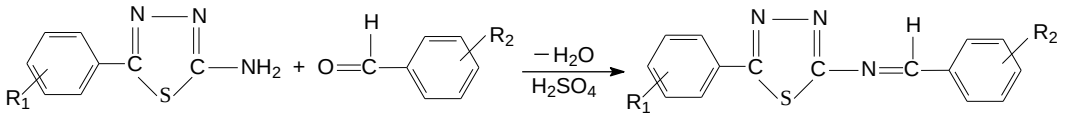

Scheme 1. Preparation of the thiadiazole Schiff base ligands (L^1–L^6). R_1=H, R_2=4-NO_2 (L^1), R_1=4-Cl, R_2= C_6H_5N (L^2), R_1=2-NO_2, R_2=2-Cl (L^3), R_1=4-OH, R_2=4-OCH_3 (L^4), R_1=4-$N(CH_3)_2$, R_2= C_6H_5N(L^5) and R_1=R_2=2-OH (L^6).

In view of the results obtained from the elemental analyses, molar conductivity, magnetic moment, IR, ^{1}H NMR, electronic, ESR, mass spectroscopy and thermal analyses, the complexation reactions were proposed to be as shown in schemes 2 and 3.

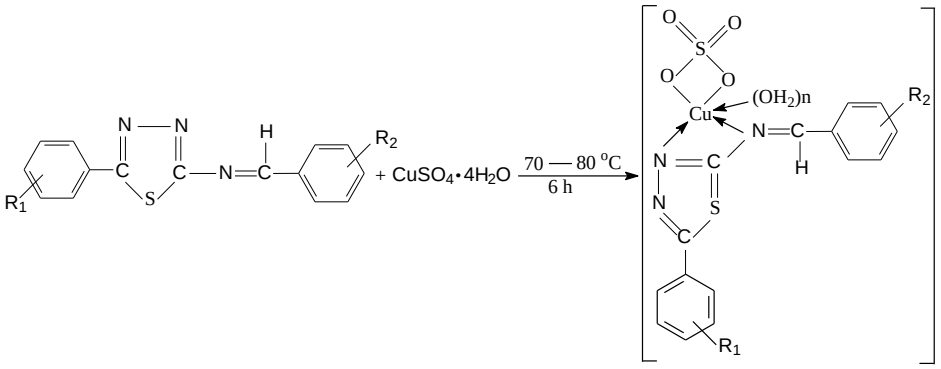

Scheme 2. Synthesis of mononuclear Cu(II) complexes (**1**-**6**). R_1=H, R_2=4-NO_2 (**1**), R_1=4-Cl, R_2= C_6H_5N (**2**), R_1=2-NO_2, R_2=2-Cl (**3**), R_1=4-OH, R_2=4-OCH_3 (**4**), R_1=4-$N(CH_3)_2$, R_2= C_6H_5N (**5**) and R_1=R_2=2-OH (**6**).

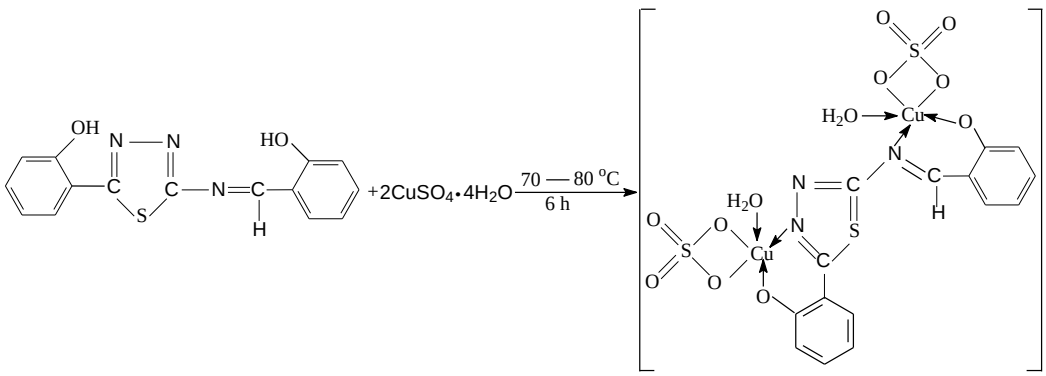

Scheme 3. Synthesis of binuclear Cu(II) complex (**7**).

3.1. Elemental analyses and molar conductance of Cu(II) complexes

The complexes obtained in this investigation are colored solids and stable towards air and moisture. They are soluble in DMF and DMSO but insoluble in water, ethanol, methanol and chloroform. The complexes were assigned to possess the composition shown in Table 2.

Table 2. Physical properties and microanalysis of Cu(II) complexes (**1-7**).

No.	Compound (Empirical formula)	M. Wt. (Cal. M. Wt.)	Color (Λ_m)	Elemental analysis			
				%C	%H	%N	%M
1	$[CuL^1(SO_4)(H_2O)_2]$ ($C_{15}H_{14}N_4CuO_8S_2$)	507.55 (506.00)	Buff (10.82)	35.24 (35.61)	2.52 (2.79)	11.35 (11.07)	12.79 (12.56)
2	$[CuL^2(SO_4)]$ ($C_{14}H_9ClCuN_4O_4S_2$)	460.40 (460.37)	Brown (12.75)	36.86 (36.53)	2.03 (1.97)	11.98 (12.17)	14.12 (13.80)
3	$[CuL^3(SO_4)(H_2O)]$ ($C_{15}H_{11}ClCuN_4O_7S_2$)	522.40 (522.39)	F. brown (12.02)	34.76 (34.49)	2.34 (2.12)	11.03 (10.73)	12.51 (12.16)
4	$[CuL^4(SO_4)(H_2O)]$ ($C_{16}H_{15}CuN_3O_7S_2$)	488.50 (488.99)	F. brown (11.79)	39.51 (39.30)	3.41 (3.09)	8.79 (8.59)	12.75 (13.00)
5	$[CuL^5(SO_4)(H_2O)]$ ($C_{16}H_{17}CuN_5O_5S_2$)	505.00 (505.02)	F. brown (11.14)	38.41 (38.05)	3.50 (3.39)	14.01 (13.87)	12.88 (12.58)
6	$[CuL^6(SO_4)(H_2O)]$ ($C_{15}H_{13}CuN_3O_7S_2$)	474.00 (474.55)	F. brown (12.64)	37.72 (37.93)	2.81 (2.76)	9.14 (8.85)	12.95 (13.38)
7	$[Cu_2L^6(SO_4)_2(H_2O)_2]$ ($C_{15}H_{15}Cu_2N_3O_{12}S_2$)	652.50 (652.57)	F. brown (11.41)	28.01 (27.61)	2.21 (2.32)	6.78 (6.44)	10.02 (9.74)

[a] All the synthesized complexes decompose with out melting above 260 °C.
The yield for the synthesized complexes was 79-85%.
M. Wt. = Molecular weight obtained from mass spectral measurements.
(Cal. M. Wt.) = Calculated molecular weight. Λ_m = Molar conductance (Ω^{-1} cm^2 mol^{-1}).

The molar conductance values for the complexes were in the range 10.82–12.64 Ω^{-1} cm^2 mol^{-1} in DMF, which denoted their non-electrolytic nature [30]. Thus, the complexes can be formulated as $[CuL(SO_4)(H_2O)_n].xH_2O$ or $[Cu_2L(SO_4)_2(H_2O)_2SO_4].xH_2O$. The obtained analytical results were consistent with the proposed molecular formula of the complexes. The following techniques were employed for the characterization of these complexes.

3.2. ESI-mass spectra

The ESI–mass spectra were measured in order to confirm the composition and the purity of the complexes under investigation (Table 1). The spectra of $[CuL^1SO_4(H_2O)_2]$ (**1**) displayed the molecular ion peak at m/z 507.55 which is attributable to $[M+1]^+$. The mass spectra of $[CuL^2SO_4]$ (**2**), $[CuL^3SO_4(H_2O)]$ (**3**), $[CuL^4SO_4(H_2O)]$ (**4**), $[CuL^5SO_4(H_2O)]$ (**5**), $[CuL^6SO_4(H_2O)]$ (**6**) and $[Cu_2L^6(SO_4)(H_2O)_2]$ (**7**) showed the highest peaks at m/z 460.40, 522.40, 488.50, 505.00, 474.00 and 652.50, respectively, corresponding to the molecular weight of the parent ion $[M]^+$ [31, 32]. These assignments are based on ^{63}Cu. Further confirmation for the molecular structure of the investigated complexes comes from the appearance of other peaks that containing ^{65}Cu besides the peaks due to

successive degradation of the target compound to various fragments [33]. Another confirmation came from the decomposition of the complexes **1**–**7** *via* the abstraction of ligands to give fragment ion peaks that is attributable to $[L]^+$ [34]. The fragmentation pattern of the Cu(II) complex **1** are shown in scheme 4. The data of the elemental analysis and MS for the prepared complexes confirm the proposed molecular formula (Table 2).

3.3. IR data

The data derived from the IR spectra of the Schiff bases are presented in Table 3.

Table 3. IR and ^{1}H NMR spectral data of the ligands (L^1-L^6) and their Cu(II) complexes (1-7).

Comp.	IR spectra (cm^{-1})						^{1}H NMR spectra (ppm)	
	$\nu(H_2O)$	ν(C=N) (Schiff)	ν(C=N) (ring)	$\nu(SO_4)$ (bidentate)	$\gamma(H_2O)$	ν(M-N)	$\delta_{Ar\text{-}H}$	$\delta_{C\underline{H}=N}$
L^1	–	1580	1515	–	–	–	7.39-8.42	10.17
1	3420	1575	1519	1119, 1032	847	507	7.75-8.78	10.53
L^2	–	1603	1524	–	–	–	7.43-8.22	9.88
2	–	1599	1486	1091, 1023	–	510	7.63-8.42	10.08
L^3	–	1612	1525	–	–	–	7.64-8.51	10.15
3	3403	1603	1521	1114, 1025	848	456	7.65-8.62	10.26
L^4	–	1580	1500	–	–	–	6.76-8.14	10.25
4	3400	1594	1467	1154, 1027	834	470	7.06-8.44	10.55
L^5	–	1585	1508	–	–	–	6.68-7.93	9.80
5	3412	1599	1523	1125, 1053	816	526	6.93-8.18	10.05
L^6	–	1590	1515	–	–	–	6.79-8.36	10.24
6	3380	1605	1513	1154, 1043	866	468	7.02-8.59	10.43
7	3370	1585	1523	1120, 1015	840	488	7.14-8.71	10.59

They showed the absence of bands due to the ν(C=O) and $\nu(NH_2)$ (present in the starting materials). Instead, a new band appeared at 1612-1580 cm^{-1} range due to the ν(HC=N) indicates the condensation of the two moieties and the formation of the Schiff bases [35]. In order to determine the binding mode of the Schiff bases to the Cu(II) in the complexes, the IR spectra of the free ligands were compared with the spectra of the complexes (Table 3). All complexes (except for **2**) showed a broad diffuse band at 3420–3370 cm^{-1} range and a low frequency band at 866–816 cm^{-1} range, revealing the presence of water molecules in the co-ordination sphere. This fact is supported by the results obtained from the elemental analysis and TGA of the complexes. IR spectra of L^6 showed a strong band at 3260 cm^{-1} that is assigned to the OH group [35]. The intensity of this band decreased in the spectra of Cu(II) complex **6** and disappeared in the spectra of Cu(II) complex **7**, indicating the coordination of the hydroxyl group through the deprotonation [36]. The shift of the azomethine stretching vibration in the complexes to the extent of 4–15 cm^{-1} indicated the co-ordination through the azomethine nitrogen [37]. Also, the band position of ν(C=N) group of the ring appeared at 1525-1500 cm^{-1} range in the spectra of the free ligands was shifted by 4-38 cm^{-1} in the spectra of the complexes, indicating the

coordination of C=N of the ring to the copper ion (except for **6**). These observations were supported by the appearance of a new non ligand band in the low frequency range (526–456 cm^{-1}) caused by the to ν(M–N). The IR spectra of complexes **6** and **7** displayed new bands at 611 and 560, respectively, corresponding to the stretching vibration of M-O [38]. IR spectra of all complexes showed new bands at 1154–1091 and 1053–1015 cm^{-1} due to the bidentate sulfate [39]. According to these observations, it can be concluded that Schiff bases L^1-L^5 coordinate in bidentate mode through nitrogen atoms of the ring and azomethine group whereas L^6 can bind to the metal ion in bi-dentate and tetra-dentate modes.

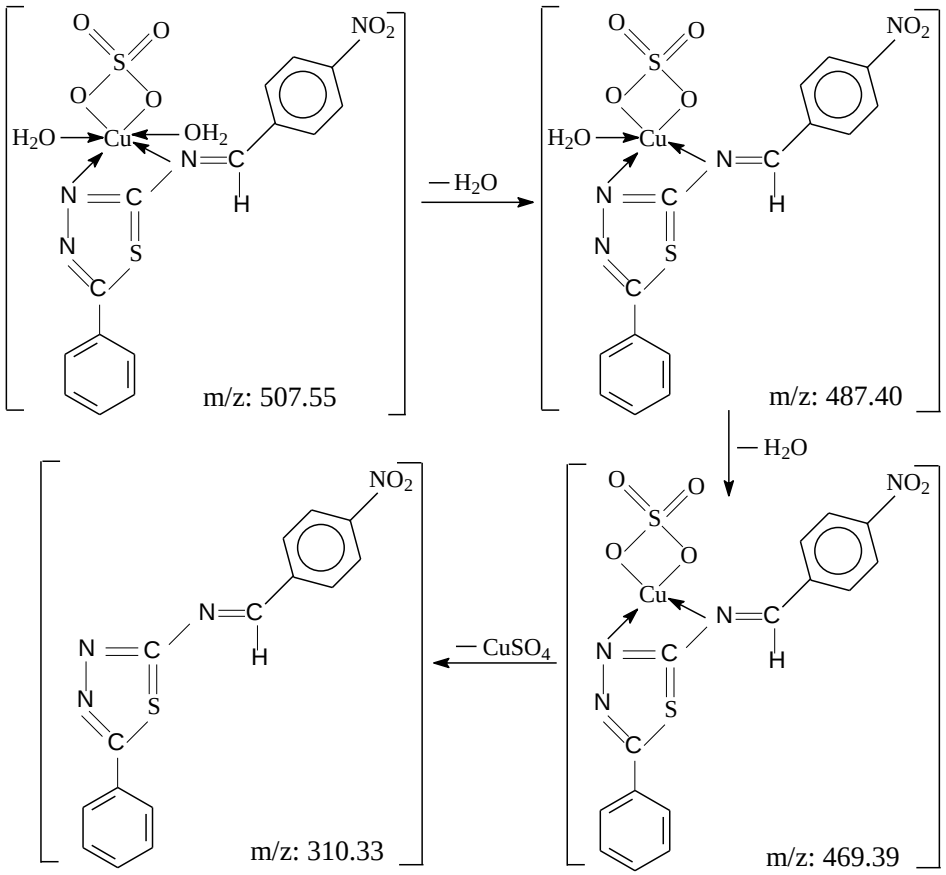

Scheme 4. Fragments observed in the mass spectrum of the Cu(II) complex 1.

3.4. ^1H NMR spectra

A Comparative study between the ^1H NMR spectra of the free ligands and those of their Cu(II) complexes **1-7** was made in order to determine the center of chelation and bonding modes in the formed chelates. The signal for the azomethine proton appearing as a singlet at 9.80-10.25 ppm in the spectra of ligands was downfield shifted in the spectra of Cu(II) complexes (Table 3). This de-shielding was attributed to the donation of the lone pair of electrons on the azomethine nitrogen to the copper ion, resulting in the formation of a coordinate bond [40]. ^1H NMR spectra of L^1-L^6 exhibited a multiplet at 6.68-8.51 ppm for hydrogens of the aromatic rings. In the spectra of Cu(II) complexes,

these peaks have downfield shifts which can be attributed to the increased conjugation upon complex formation [33]. The intensity of the signal observed at 11.36 ppm due to δ_{OH} in spectra of L^6 disappeared in the spectra of Cu(II) complexes **6** and **7**. This refers to the complex formation occurring *via* the deprotonation of the OH group [41]. The changes and downfield shifts in the spectra of copper complexes are good indications for participation of these groups in the coordination with the metal ions, and give further support for the presence of the metal ions. Similar viewpoints on ^{1}H NMR spectral studies of paramagnetic Cu(II)-complexes have been reported by Wang and Ma [42]. Khedr *et al*. have studied the ^{1}H NMR spectra of the paramagnetic Mn(II), Co(II), Ni(II) and Cu(II) complexes [19, 33]. Also, ^{1}H NMR spectral studies of paramagnetic Fe(II) complexes have been reported by Wu *et al*. [43].

3.5. Electronic spectra and magnetic moment measurements

Table 4. UV-Vis, ESR spectra and magnetic moment data of the ligands (L^1-L^6) and their Cu(II) complexes (**1-7**).

Comp.	UV-Vis spectra (λ_{max} nm)		ESR spectra				μ_{eff} (B.M.)	Geometry
	Intra-ligand transitions	d-d transitions	g_{ll}	$g_{\perp}$	g_{av}	G		
L^1	210, 260	–	–	–	–	–	–	–
1	270, 320	360, 560	g_{iso} = 2.173				1.76	Octahedral
L^2	220, 330	–	–	–	–	–	–	–
2	270, 340	370, 510	2.344	2.105	2.186	3.276	1.86	square planar
L^3	207, 300	–	–	–	–	–	–	–
3	265, 345	525	---	---	---	---	1.74	Square pyramidal
L^4	216, 320	–	–	–	–	–	–	–
4	290, 340	510	---	---	---	---	1.76	Square pyramidal
L^5	228, 345	–	–	–	–	–	–	–
5	260, 360	515	2.296	2.102	2.168	2.902	1.73	Square pyramidal
L^6	218, 290	–	–	–	–	–	–	–
6	270, 330	530	---	---	---	---	1.72	Square pyramidal
7	260, 333	532	---	---	---	---	1.75	Square pyramidal

--- = Not determined. μ_{eff} = Magnetic moment.

The electronic spectra of the free ligands and their Cu(II)-complexes as well as the magnetic moments (μ_{eff}/B.M.) per metal atom were measured at room temperature (Table 4). The free ligands displayed absorption bands within the 207-228 and 260-345 nm ranges. The shorter wavelength band attributed to the high energy π—π* transition corresponds to the ^1L_a—^1A state in the aromatic moiety [44]. The longer wavelength band was assigned to the n—π* transition within the CH=N group [45]. In the spectra of complexes, the former transition underwent a red shift and the latter is replaced by an intense absorption bands within the 320-360 nm range. This band may be assigned to the t_2(M)→π*(L) charge transfer transition. The electronic spectrum of the Cu(II) complex **1** showed two ligand field bands at 560 and 360 nm. These bands are assigned to the transitions $^2T_{2g}$→^2E_g and charge transfer, respectively, and denote an octahedral geometry [46]. Cu(II) complex **1** exhibited a magnetic moment

value of 1.79 B.M., which confirms an octahedral geometry around the central metal ion [47]. Complex **2** displayed two bands at 370 and 510 nm. They correspond to the ligand→metal charge transfer and the $^2B_{1g}\rightarrow{}^2B_{2g}$ transitions for Cu(II) ion in a square planar geometry [48]. The magnetic moment of the Cu(II) complex **2** was 1.86 B.M., which supports its square planar geometry [48]. Cu(II) complexes **3-7** exhibited asymmetric absorption bands within the 510-532 nm range. These bands are attributed to the $d(x^2\text{-}y^2)\rightarrow(d_{xz}, d_{yz})$ transition which is compatible with complexes having square pyramidal structure [49]. The room temperature magnetic moments of Cu(II) complexes **3-7** lies within the 1.72-1.76 B.M. range, which almost agree with the spin value of 1.73 for S = ½, as usually observed for Cu(II) complexes.

3.6. Electron spin resonance spectra

X-band ESR spectra of the powder samples of Cu(II) complexes **1**, **2** and **5** exhibited axial patterns with two g values at 303 K (Figure 1). The $g_{\|}$ and $g_{\perp}$ values are > 2.04 (Table 3), which is consistent with the elongated tetragonally distorted and distorted square-based pyramidal copper(II) complexes with all the principle axes aligned parallel [50]. The fact that $g_{\|} > g_{\perp} > g_e$ (2.0023), showed that the unpaired d-electron is in the $dx^2\text{-}y^2$ orbital of Cu(II) and the spectral features are characteristics of axial symmetry [51]. The G factor, defined as $G = (g_{\|}-2) / (g_{\perp}-2)$ is < 4.00, suggesting the existence of an interaction between Cu(II) centers in the solid state. The local axes are appreciably misaligned and the energies of the electronic transitions involved were comparable [52]. Such stereo-chemistries probably arise from the bulkiness of the in-plane ligands which impose strain in the chelation sites. Cu(II) complex **1** exhibited an isotropic spectrum with an intense broad signal, but no hyperfine structure owing to the dipolar broadening and unresolved hyperfine interactions [53]. The g_{iso} value, 2.173, suggested a geometry containing grossly misaligned tetragonal axes [54].

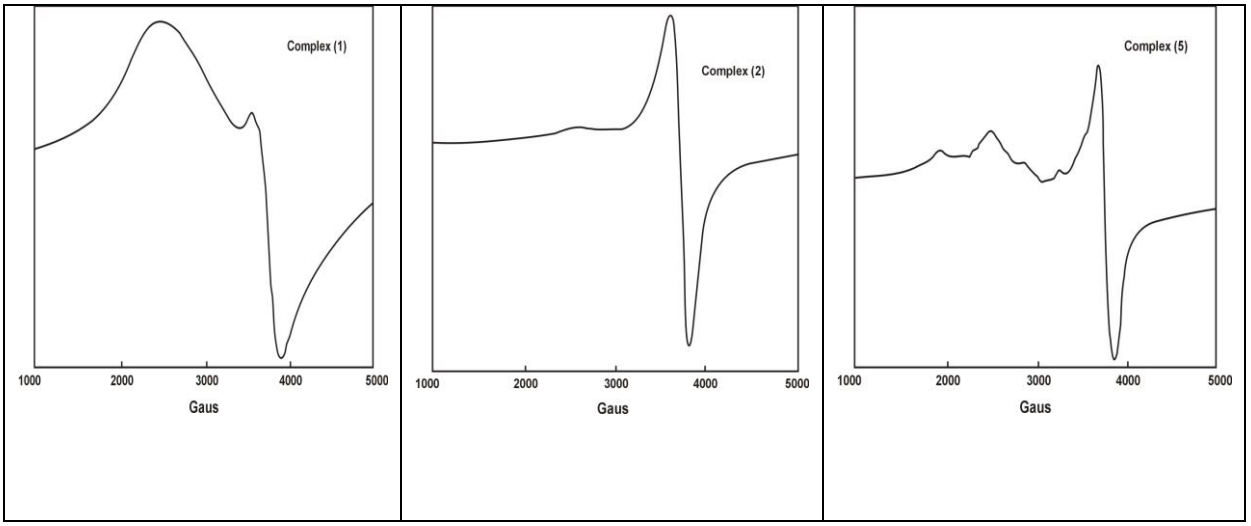

Figure 1. X-band ESR spectra of solid Cu(II) complexes **1**, **2** and **5** at 303 K.

3.7. Thermal analyses (DTA and TGA)

From thermal analysis, the properties, nature of intermediates and final products of the thermal decomposition of coordination compounds can be obtained [55]. From TGA curves, the mass loss was calculated for the different steps and compared with those theoretically calculated for the suggested formulae based on the results of elemental analyses and MS together with the molar conductance measurements. The TGA confirms the formation of CuO or $CuSO_4$ as the end products from which the metal content could be calculated and compared with that obtained from the analytical determination. The found and calculated mass losses, relative residues and temperature observed in each step of TGA/DTA curves are given in Table 5.

Table 5. TGA and DTA data of Cu(II) complexes 1-7.

Comp.	Step	TGA		Assignment (thermal process)	DTA	
		Temperature range (ºC)	% Weight loss [found (Calcd)]		Temperature range (ºC)	peaks
1	1st	120-160	7.00 (7.12)	Elimination of two coordinated water molecules	125-165	Endo.
	2nd	170-300	23.98 (24.13)	Partial decomposition of the complex.	165-290	Exo.
	3rd	310-750	37.50 (37.20)	Complete decomposition of the complex and formation of $CuSO_4$ as a final product	305-740	Exo.
2	1st	200-250	25.00 (24.46)	Partial decomposition of the complex.	190-240	Exo.
	2nd	260-770	57.76 (58.26)	Complete decomposition of the complex and formation of CuO as a final product	250-760	Exo.
3	1st	120-170	2.89 (3.45)	Elimination of one coordinated water molecule	125-175	Endo.
	2nd	180-290	23.86 (23.37)	Partial decomposition of the complex.	170-285	Exo.
	3rd	300-710	57.55 (57.95)	Complete decomposition of the complex and formation of CuO as a final product	290-700	Exo.
4	1st	120-150	3.70 (3.68)	Elimination of one coordinated water molecule	125-160	Endo.
	2nd	170-270	19.12 (18.81)	Partial decomposition of the complex.	160-280	Exo.
	3rd	280-295	60.99 (61.25)	Complete decomposition of the complex and formation of $CuSO_4$ as a final product	275-305	Exo.

The results showed that Cu(II) complexes **1-7** decompose mainly in three steps. The first step appeared within the temperature range 120-170ºC (Figure 2) was due to the elimination of coordinated water molecules [56]. This appeared as an endothermic peak in the DTA curves within the temperature range 125-175ºC. The Cu(II) complex **2** exhibits thermal stability up to 200 ºC, which confirms that this complex is free from any types of water molecules [56]. The second step within the temperature range 170-430ºC was associated with an exothermic DTA peak at 160-440ºC range. This peak was due to the partial decomposition of the ligand. The final decomposition step appeared above 260ºC corresponding to the complete thermal decomposition of the complexes and the loss of their organic portion resulting in the formation of CuO or $CuSO_4$ as final products. This last step appeared as an

exothermic peak in the DTA curves at 250-790ºC range, confirming the data obtained from the TGA curves.

Table 5. *Continued*.

Comp.	Step	TGA		Assignment (thermal process)	DTA	
		Temperature range (ºC)	% Weight loss [found (Calcd)]		Temperature range (ºC)	peaks
5	1st	130-170	3.50 (3.57)	Elimination of one coordinated water molecule	125-165	Endo.
	2nd	190-290	23.92 (23.80)	Partial decomposition of the complex.	180-285	Exo.
	3rd	300-795	41.23 (41.03)	Complete decomposition of the complex and formation of $CuSO_4$ as a final product	290-790	Exo.
6	1st	125-165	3.80 (3.79)	Elimination of one coordinated water molecule	130-170	Endo.
	2nd	180-430	62.11 (62.11)	Partial decomposition of the complex.	175-420	Exo.
	3rd	440-560	17.30 (16.85)	Complete decomposition of the complex and formation of CuO as a final product	445-570	Exo.
7	1st	128-170	5.42 (5.52)	Elimination of two coordinated water molecules	125-165	Endo.
	2nd	185-435	45.75 (45.56)	Partial decomposition of the complex.	180-430	Exo.
	3rd	450-565	25.00 (24.54)	Complete decomposition of the complex and formation of CuO as a final product	440-560	Exo.

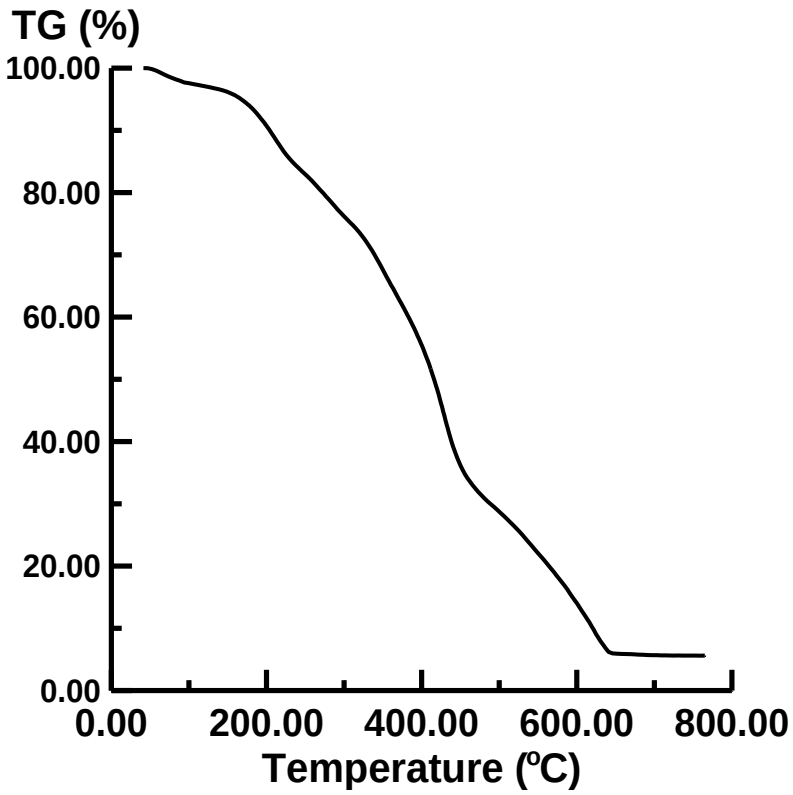

Figure 2. TGA curve of $[CuL^5(SO_4)(H_2O)]$ (**5**).

3.8. 3D molecular modeling and analysis

Because the single crystals could not be obtained for these complexes, it was thought worthwhile to obtain structural information. Molecular modeling studies of a representative complex **2** were carried out. All calculations were performed using CS Chem 3-D Ultra Molecular Modeling and Analysis Program [17].

Table 6. Various bond lengths of compound $[CuL^2(SO_4)]$ (**2**)

No.	Atoms	Actual bond lengths	Optimal bond lengths	No	Atoms	Actual bond lengths	Optimal bond lengths
1	C(1)-N(2)	1.332	1.260	21	S(11)-C(14)	1.723	1.856
2	C(1)-C(6)	1.399	1.503	22	N(12)-N(13)	1.358	—
3	C(1)-H(30)	1.102	1.100	23	N(13)-C(14)	1.298	1.260
4	N(2)-C(3)	1.362	1.456	24	C(14)-C(15)	1.474	1.503
5	C(3)-C(4)	1.413	1.503	25	C(15)-C(16)	1.403	1.420
6	C(3)-C(7)	1.443	1.337	26	C(15)-C(20)	1.406	1.420
7	C(4)-C(5)	1.395	1.420	27	C(16)-C(17)	1.398	1.420
8	C(4)-H(35)	1.098	1.100	28	C(16)-H(34)	1.102	1.100
9	C(5)-C(6)	1.394	1.420	29	C(17)-C(18)	1.395	1.420
10	C(5)-H(28)	1.102	1.100	30	C(17)-H(32)	1.102	1.100
11	C(6)-H(29)	1.101	1.100	31	C(18)-C(19)	1.398	1.420
12	C(7)-N(8)	1.389	1.462	32	C(18)-Cl(21)	1.725	1.719
13	C(7)-H(27)	1.105	1.100	33	C(19)-C(20)	1.395	1.420
14	N(8)-Cu(9)	1.838	—	34	C(19)-H(31)	1.102	1.100
15	N(8)-C(10)	1.415	1.462	35	C(20)-H(33)	1.101	1.100
16	Cu(9)-N(12)	1.838	—	36	O(22)-S(24)	1.724	—
17	Cu(9)-O(22)	1.798	—	37	O(23)-S(24)	1.725	—
18	Cu(9)-O(23)	1.797	—	38	S(24)-O(25)	1.453	1.450
19	C(10)-S(11)	1.794	1.856	39	S(24)-O(26)	1.452	1.450
20	C(10)-N(12)	1.438	1.377				

It is an interactive graphics program that allows rapid structure building, geometry optimization with minimum energy and molecular display. It has ability to handle transition metal and inner transition metal complexes [18-21]. It enables the calculation of the actual bond lengths, angles and total static energy of a molecule in terms of deviations from reference unstrained bond lengths, angles, and torsions plus non-bonded interactions. In view of the tetra-coordination of the Cu(II) complex, $[CuL^2(SO_4)]$ (**2**) (vide analytical studies), the molecular modeling of this compound is based on its square planar structure. The correct stereochemistry was assured through, manipulation and modification of the molecular coordinates to obtain reasonable and low energy molecular geometries. Energy minimization was repeated several times to find the global minimum [21]. In all 104 measurements of bond lengths (39 in numbers) and the bond angles (65 in numbers) are given in Tables 6 and 7. Except for a few cases, the optimal values (most favorable) of both the bond lengths and the bond angles are given in the Tables along with the actual ones. In most of the cases, the actual bond lengths and bond angles are close to the optimal values, and thus the proposed structure of the complex **2** and other complexes are acceptable.

Table 7. Various bond angles of compound [$CuL^2(SO_4)$] (**2**)

No.	Atoms	Actual bond angle	Optimal bond angle	No.	Atoms	Actual bond angle	Optimal bond angle
1	N(2)-C(1)-C(6)	123.907	123.500	34	Cu(9)-N(12)-N(13)	119.773	—
2	N(2)-C(1)-H(30)	116.222	116.500	35	C(10)-N(12)-N(13)	111.880	—
3	C(6)-C(1)-H(30)	119.872	120.000	36	N(12)-N(13)-C(14)	117.561	—
4	C(1)-N(2)-C(3)	119.597	115.000	37	S(11)-C(14)-N(13)	112.297	126.000
5	N(2)-C(3)-C(4)	119.473	120.000	38	S(11)-C(14)-C(15)	124.281	119.000
6	N(2)-C(3)-C(7)	114.796	120.000	39	N(13)-C(14)-C(15)	123.407	120.000
7	C(4)-C(3)-C(7)	125.730	120.000	40	C(14)-C(15)-C(16)	120.190	120.000
8	C(3)-C(4)-C(5)	120.558	120.000	41	C(14)-C(15)-C(20)	121.837	120.000
9	C(3)-C(4)-H(35)	122.528	120.000	42	C(16)-C(15)-C(20)	117.924	120.000
10	C(5)-C(4)-H(35)	116.913	120.000	43	C(15)-C(16)-C(17)	121.184	120.000
11	C(4)-C(5)-C(6)	118.788	120.000	44	C(15)-C(16)-H(34)	120.672	120.000
12	C(4)-C(5)-H(28)	120.758	120.000	45	C(17)-C(16)-H(34)	118.133	120.000
13	C(6)-C(5)-H(28)	120.454	120.000	46	C(16)-C(17)-C(18)	119.989	120.000
14	C(1)-C(6)-C(5)	117.671	120.000	47	C(16)-C(17)-H(32)	119.409	120.000
15	C(1)-C(6)-H(29)	121.205	120.000	48	C(18)-C(17)-H(32)	120.602	120.000
16	C(5)-C(6)-H(29)	121.123	120.000	49	C(17)-C(18)-C(19)	119.669	120.000
17	C(3)-C(7)-N(8)	131.373	119.000	50	C(17)-C(18)-Cl(21)	120.172	118.800
18	C(3)-C(7)-H(27)	118.127	120.000	51	C(19)-C(18)-Cl(21)	120.158	118.800
19	N(8)-C(7)-H(27)	110.470	113.500	52	C(18)-C(19)-C(20)	120.033	120.000
20	C(7)-N(8)-Cu(9)	115.257	—	53	C(18)-C(19)-H(31)	120.559	120.000
21	C(7)-N(8)-C(10)	118.606	124.000	54	C(20)-C(19)-H(31)	119.408	120.000
22	Cu(9)-N(8)-C(10)	91.987	—	55	C(15)-C(20)-C(19)	121.161	120.000
23	N(8)-Cu(9)-N(12)	74.390	—	56	C(15)-C(20)-H(33)	121.020	120.000
24	N(8)-Cu(9)-O(22)	122.829	—	57	C(19)-C(20)-H(33)	117.818	120.000
25	N(8)-Cu(9)-O(23)	123.451	—	58	Cu(9)-O(22)-S(24)	86.411	—
26	N(12)-Cu(9)-O(22)	124.520	—	59	Cu(9)-O(23)-S(24)	86.424	—
27	N(12)-Cu(9)-O(23)	124.848	—	60	O(22)-S(24)-O(23)	96.111	—
28	O(22)-Cu(9)-O(23)	91.053	—	61	O(22)-S(24)-O(25)	110.277	—
29	N(8)-C(10)-S(11)	109.173	—	62	O(22)-S(24)-O(26)	110.675	—
30	N(8)-C(10)-N(12)	102.332	—	63	O(23)-S(24)-O(25)	110.367	—
31	S(11)-C(10)-N(12)	107.176	—	64	O(23)-S(24)-O(26)	110.587	—
32	C(10)-S(11)-C(14)	90.705	98.500	65	O(25)-S(24)-O(26)	116.883	116.600
33	Cu(9)-N(12)-C(10)	91.240	—				

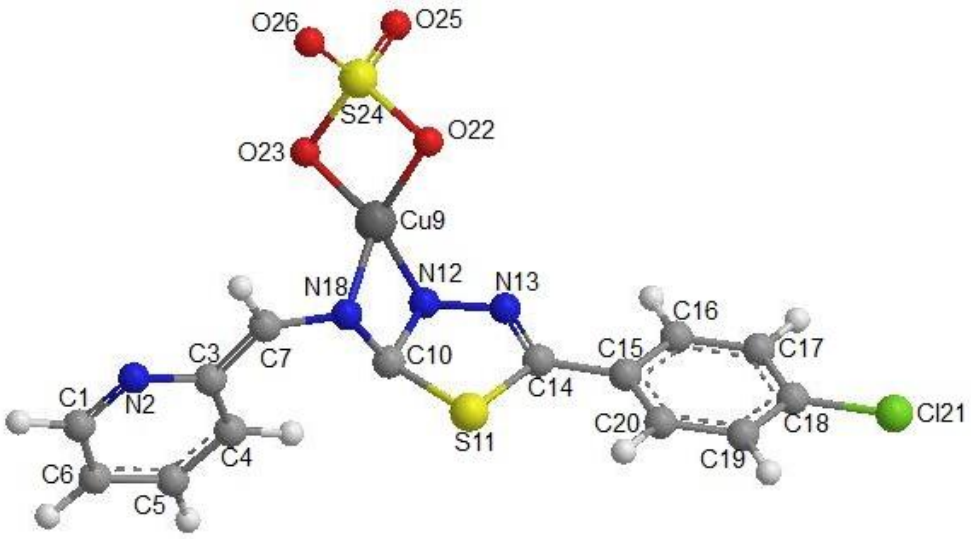

Figure 3. 3D structure of [$CuL^2(SO_4)$] (**2**).

All theoretically calculated coordinative covalent bond lengths and bond angles are in accordance with the square planer geometry (Figure 3). The energy minimization value for square planar structure of the Cu(II)-complex **2** is 92.0 Kcal/mol.

3.9. In-vitro antimicrobial assay

Table 8. Antimicrobial activities of the ligands (L^1-L^6) and their Cu(II) complexes (**1**-**7**).

Compound	Inhibition zone diameter (mm/mg sample) [a]			
	Escherichia coli (G^-)	*Staphylococcus aureus* (G^+)	*Aspergillus flavus* (Fungus)	*Candida albicans* (Fungus)
Control: DMSO	0.0	0.0	0.0	0.0
Tetracycline (Antibacterial agent)	33.0 ± 0.3	30.0 ± 0.4	---	---
Amphotericin B (Antifungal agent)	---	---	20.0 ± 0.2	20.0 ± 0.1
L^1	14 ± 0.2	12 ± 0.1	10 ± 0.3	11 ± 0.2
1	15 ± 0.4	13 ± 0.2	11 ± 0.1	17 ± 0.3
L^2	13 ± 0.3	13 ± 0.4	0.0	12 ± 0.2
2	18 ± 0.1	14 ± 0.3	12 ± 0.2	13± 0.3
L^3	11 ± 0.2	0.0 ± 0.2	0.0	0.0
3	15 ± 0.3	17 ± 0.4	10 ± 0.2	11 ± 0.1
L^4	12 ± 0.2	12 ± 0.1	0.0	0.0
4	14 ± 0.4	15 ± 0.4	10.0 ± 0.1	12 ± 0.3
L^5	10 ± 0.1	10 ± 0.1	0.0	12 ± 0.2
5	11 ± 0.3	12 ± 0.2	10. ± 0.3	11± 0.2
L^6	14 ± 0.2	18 ± 0.4	0.0	9 ± 0.1
6	19 ± 0.3	20 ± 0.2	0.0	12 ± 0.3
7	23 ± 0.4	26 ± 0.3	16 ± 0.3	14 ± 0.2

[a] Each experiment has been conducted three times at least.

It was reported that coordination compounds were characterized by their antitumor, antiviral and antimalarial activities. These characteristic properties were related to the ability of the metal ion to form complexes with ligand containing sulfur, nitrogen and oxygen donor atoms [57]. The synthesized ligands and their complexes were screened for their antibacterial activity against *E. coli* and *S. aureus* and antifungal activity against *A. flavus* and *C. albicans*. The standard drugs tetracycline and amphotericin B were also tested for their antibacterial and antifungal activities at the same concentration and conditions similar to that of the tested compounds concentration. The antimicrobial results were presented in Table 8. From the antibacterial studies, it is inferred that the Schiff bases and their Cu(II) complexes were found to be potentially active against *A. flavus* and *C. albicans*. In case of antifungal activity, the Schiff bases L^2-L^6 were found to be inactive against *A. flavus* whereas Schiff bases L^3 and L^4 were inactive against *C. albicans*. On the other hand, all Cu(II) complexes under investigation exhibited moderate activity against *A. flavus* and *C. albicans* except for complex **6**, which was inactive against *A. flavus*.

From the obtained results, it can be observed that the complexes showed greater activity as compared to the Schiff base. The improved activities of the metal complexes as compared to the ligand

can be explained on the basis of chelation theory [58]. This theory explains that a decrease in the polarizability of the metal could enhance the lipophilicity of the complexes, which leads to a breakdown of the permeability of the cells, resulting in interference with normal cell processes [59]. This indicates that the chelation tends to make the Schiff base act as more powerful and potent antimicrobial agents, thus inhibiting the growth of bacteria and fungi more than the parent Schiff bases [60, 61]. For binuclear Cu(II) complex **7**, its activity was tested at the same Cu(II) concentration as that of mononuclear counterparts. The data in Table 8 indicates that the binuclear Cu(II) complex **7** is more active than mononuclear Cu(II) complex **6**, which means that the antimicrobial activity increases with increasing the number of metal ions per complex for the same ligand at the same concentration of Cu(II) ions. Therefore, it is claimed that the process of chelation dominantly affects the biological behavior of the compounds that are potent against microbial and fungal strains. From these studies, it is also proposed that the percentage ratio of the metal ions and the geometry of the complexes play a significant role in the biological behavior of the metal chelates. It is suspected that factors such as solubility, different dipole moment and cell permeability mechanisms may be influenced by the presence of the different geometries and ratios of metal ions, which in turn affect the overall mechanism of permeation through the lipoid layer of the organisms thus killing them more effectively and efficiently [62].

In comparison with other publications discussed the biological activity of copper-thiadiazole complexes as fungicidal [62] or bactericidal [63, 64] agents, we have selected *S. aureus* to represent gram positive bacteria and *E. coli* as the backbone of gram negative bacteria. Also, we selected *C. albicans* to represent the unicellular fungi and *A. flavus* as a higher fungus, which represents multicellular fungi. Hence, the tested bacteria and fungi represent a broad spectrum of the test organisms. The obtained data proved the potential usefulness of the present Cu(II)-complexes as broad spectrum antimicrobial agents.

3.10. Catalytic effect of Cu(II)-Schiff base complexes on the cathodic reduction of oxygen

The catalytic effect of the Cu(II)-complexes on the cathodic reduction of oxygen at a glassy carbon electrode was studied in 2.0 M phosphoric acid. The solution was saturated with air by bubbling a fine stream of air for ≈ 40 min. The cathodic reduction of oxygen was carried out, then increasing volumes (0.1-3.0 mL) of $2x10^{-4}$ M solution of the Cu(II) complexes were added and the voltamogram was recorded. The concentration ranges used were chosen as not to give reduction peaks for Cu(II) or Schiff base at the electrode surface. The addition of the Cu(II) complexes caused obvious changes in the CV curves which can be summarized as follows:

a. The reduction of oxygen gave a single cathodic peak with E_P=-1.10 volt vs. Ag/AgCl electrode in the absence of catalysts but no anodic ones are observed denoting that the reduction proceeds irreversibly. The addition of the complexes causes a shift of E_P to less negative potentials and the peak current (i_P) increased to some extent (Table 9 and Fig. 4).

Table 9. Catalytic effect of the Cu(II)-complexes **(3** and **6).**

Complex No.	Conc. of Comp. (M)	ΔE_p (O_2) [mV]	ΔE_p (H_2) [mV]
(3)	$1x10^{-6}$	80	70
	$1x10^{-5}$	132	154
	$1x10^{-4}$	140	160
(6)	$1x10^{-6}$	132	66
	$1x10^{-5}$	154	176
	$1x10^{-4}$	280	280

b. The magnitude of shift in E_P and rise in i_P increased with increasing the concentrations of the catalyst (Table 10) which is more obvious at lower concentrations. The plot of ΔE_P or Δi_P as a function of complex concentration gave an almost sigmoid curve.

Table 10. Effect of the Cu(II)-complex (**4**) concentration on the catalytic reduction of oxygen.

Conc. (mg/L)	i_P (μA)	E_p (V)	ΔE_p (V)
0.0	13.85	0.720	----
2.2	14.50	0.550	0.170
3.3	15.00	0.520	0.200
5.3	16.90	0.500	0.220
11.3	19.20	0.475	0.245

c. The shift in E_P is higher than those observed with Schiff bases complexes in previous studies [65] denoting that the investigated complexes are more efficient catalysts for oxygen reduction. For the concentration range studied, the maximum shift in case of metal complexes in previous studies was 190 mV while of Cu(II)-complexes under interest it reached 280 mV.

d. The shift of E_P to less negative potential in presence of Cu(II)-complexes denotes that these complexes catalyze the oxygen reduction by decreasing the activation energy of the electrode reaction.

e. The increase in i_P values can be expressed by assuming that the catalyst can have one of the following functions or both:

i) The electrode reaction in absence of catalyst would involve the reduction of oxygen to water (four electron process) accompanied with the reduction to hydrogen peroxide (two electron process).

$$O_2 + 4e^- + 4H^+ \rightarrow H_2O \qquad (1)$$

$$O_2 + 2e^- + 2H^+ \rightarrow H_2O_2 \qquad (2)$$

The presence of the catalyst would favour the first reaction at the expense of the second one, hence, the number of electrons consumed in the electrode process increases leading to a higher i_P value.

ii) The increase in current in the presence of the catalyst can be ascribed to increased amount of oxygen transferred to the electrode surface; under conditions in which Cu(II) complexes act as oxygen carrier. The magnitude of shift in E_P and i_P depends on the molecular structure of the catalyst used.

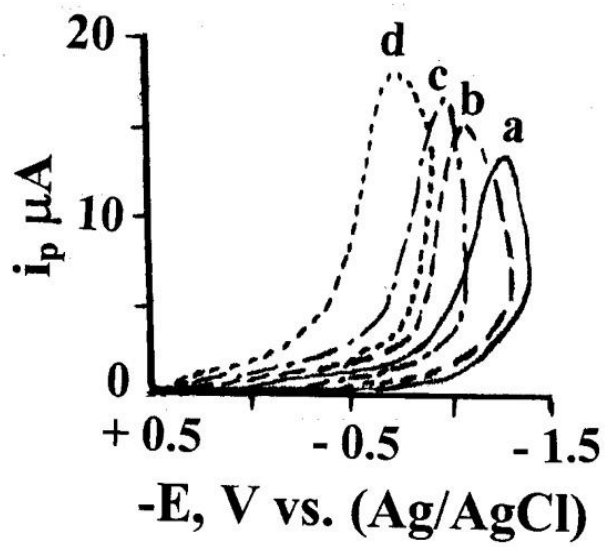

Figure 4. Cyclic voltammograms of oxygen reduction at glassy carbon electrode at different concentrations of Cu(II)-complex (**5**). (**a**) Free oxygen. (**b**) At Cu(II)-complex (**5**) conc. = 1 μg ml^{-1}.(**c**) At Cu(II)-complex (**5**) conc. = 2 μg ml^{-1}. (**d**) At Cu(II)-complex (**5**) conc. = 1 μg ml^{-1}.

4. CONCLUSION

Seven mono and binuclear Cu(II) complexes with new Schiff bases derived from 2-amino-5-substituted-aryl-1,3,4-oxadiazole (L^1–L^6) were synthesized and characterized by elemental and thermal analyses, spectral, and magnetic data. The IR, ^{1}H NMR, and UV-Vis spectra revealed that L^1–L^6 coordinate in bidentate or tetradentate modes to Cu(II) ions forming octahedral, square planar or square pyramidal complexes. Mass spectra under EI-conditions are in agreement with the elemental analyses, confirming the compositions and purities of the Cu(II) complexes. The proposed structures of the investigated complexes were supported by 3-D molecular modeling of complex **2** as a representative compound. In most cases, the ligands and complexes were active against bacteria (*E. coli* and *S. aureus*) and fungi (*A. flavus* and *C. albicans*), thus giving a new thrust of these compounds in the field of metallo-drugs (bio-inorganic chemistry). Metallization increased the activity compared with the free ligand. The binuclear complex has higher activity than the mononuclear ones. The investigated complexes have high catalytic activity towards the cathodic reduction of oxygen.

ACKNOWLEDGEMENT
This paper was funded by the Deanship of Scientific Research (DSR), King Abdulaziz University, Jeddah, under grant No. (92-130-D1432). The authors, therefore, acknowledge with thanks DSR technical and financial support.

References

1. F.D. Karia, P.H. Parsania. *Asian J. Chem.* 11 (1999) 991.
2. C.R. Choudhury, S.K. Mondal, S. Mitrra, S.D.G. Mahali, K.M.A. Malik. *J. Chem. Crytallogr.* 31 (2002) 57.
3. M.S. Alexandre-Moreira, M.R. Piuvezam, C.C. Araújo, G. Thomas. *J. Ethnopharmacol*. 67 (1999) 171.
4. S.N. Sawhney, A. Gupta, P.K. Sharma. *İndian J. Heterocycl. Chem.* 1 (1991) 8.
5. A. Foroumadi, S. Mansouri, Z. Kirani, A. Rahman. *Eur. J. Med. Chem.* 38 (2003) 851.
6. R.K. Khare, H. Sing, A.K. Srivastava. *Indian J. Chem.* 46B (2007) 875.
7. M. Amir, K. Shikha. *Eur. J. Med. Chem.* 39 (2004) 535.
8. M.D. Mullican, M.W. Wilson, D.T. Connor, C.R. Konstlan, D.J. Schrier, R.D. Dyer. *J. Med. Chem.* 36 (1993) 1090.
9. K. Srivastava, S.N. Pandeya. *Bioorg. Med. Chem.* 3 (1993) 547.
10. J. Matysiak. *Eur. J. Med. Chem.* 42 (2007) 940.
11. B.H. Lee, F.E. Dutton, M.F. Clothier, J.W. Bowman, J.P. Davis, S.S. Johnson, E.M. Thomas, M.R. Zantello, E.W. Zinser, J.C. McGuire, D.P. Thompson, T.G. Geary. *Bioorg. Med. Chem. Lett.* 9 (1999) 1727.
12. S. Schenone, O. Bruno, A. Ranise. *Bioorg. Med. Chem.* 9 (2001) 2149.
13. M. Bulbul, N. Sarcoglu. *Bioorg. Med. Chem.* 10 (2002) 2561.
14. E.E. Oruç, S. Rollas, F. Kandemirli, N. Shvets, A.S. Dimoglo. *J. Med. Chem.* 47 (2004) 6760.
15. A.I. Vogel. *A Text Book of Quantitative Inorganic Analysis*, 3rd Edt., Longmans, London (1975).
16. M. Carcelli, S. Ianelli, P. Pelogatti, G. Pelizzi, D. Rogolino, C. Solians, M. Tegoni. *Inorg. Chim. Acta* 358 (2005) 903.
17. CS Chem 3D Ultra Molecular Modeling and Analysis, Cambridge. Available online at: www.cambridgesoft.com.
18. R.C. Maurya, S. Rajput. *J. Mol. Struct.* 794 (2006) 24.
19. A.M. Khedr, N.A. El-Wakiel, S. Jadon, V. Kumar. *J. Coord. Chem.* 64 (2011) 851.
20. A.M. Khedr, S. Jadon, V. Kumar. *J. Coord. Chem.* 64 (2011) 1351.
21. B.K. Singha, H.K. Rajourb, A. Prakasha, N. Bhojakc. *Global J. Inorg. Chem.* 1 (2010) 65.
22. A.W. Bauer, W.M. Kirby, C. Sherris, M. Turck. *Am. J. Clin. Path.* 45 (1966) 493.
23. M.A. Pfaller, L. Burmeister, M.A. Bartlett, M.G. Rinaldi. *J. Clin. Microbiol*. 26 (1988) 1437.
24. National Committee for Clinical Laboratory Standards. Performance Antimicrobial Susceptibility of Flavobacteria, Vol. 41 (1997).
25. National Committee for Clinical Laboratory Standards. Reference Method for Broth Dilution Antifungal Susceptibility Testing of Conidium-forming Filamentous Fungi: Proposed Standard M38-A, NCCLS, Wayne, PA, USA (2002).
26. National Committee for Clinical Laboratory Standards. Method for Antifungal Disk Diffusion Susceptibility Testing of Yeast: Proposed Guideline M44-P, NCCLS, Wayne, PA, USA (2003).
27. National Committee for Clinical Laboratory Standards. Methods for Dilution Antimicrobial Susceptibility Tests for Bacteria that Grow Aerobically. Approved standard M7-A3, NCCLS, Villanova, PA (1993).
28. L.D. Liebowitz, H.R. Ashbee, E.G.V. Evans, Y. Chong, N. Mallatova, M. Zaidi, D. Gibbs. *Diagn. Microbiol. Infect. Dis*. 4 (2001) 27.
29. M.J. Matar, L. Ostrosky-Zeichner, V.L. Paetznick, J.R. Rodriguez, E. Chen, J.H. Rex. *Antimicrob. Agents Chemother*. 47 (2003) 1647.
30. B.K. Kumar, V. Ravinder, G.B. Swamy, S.J. Swamy. *Indian J. Chem*. 33A (1994) 136.
31. Y. Wang, G. Lin, J. Hong, L. Li, Y. Yang, T. Lu. *J. Coord. Chem.* 63 (2010) 3662.
32. F. Firdaus, K. Fatma, M. Azam, M. Shakir. *J. Coord. Chem.* 63 (2010) 3956.
33. A.M. Khedr, D.F. Draz. *J. Coord. Chem.* 63 (2010) 1418.

34. B.K. Singh, P. Mishra, B.S. Garg. *Transition Met. Chem*. 32 (2007) 603.
35. Y. Prashanthi, K. Kiranmai, N.J.P. Subhashini, Shivaraj. *Spectrochim. Acta A* 70 (2008) 30.
36. E. Canpolat, M. Kaya. *Russ. J. Coord. Chem*. 31 (2005) 415.
37. E. Canpolat. *Polish J. Chem*. 79 (2005) 619.
38. K. Nakamoto. *Infrared Raman Spectra of Inorganic and Coordination Compounds*, 3rd Edt., John Wiley and Sons, New York (1992).
39. T. Rosu, S. Pasculescu, V. Lazar, C. Chifiriuc, R. Cernat. *Molecules* 11 (2006) 904.
40. A. Varshney, J.P. Tandon, A.J. Crowe. *Polyhedron* 5 (1986) 739.
41. S.C. Chaudhry, C. Verma, S.S. Bhatt, N. Sharma. *Synth. React. Inorg. Met.-Org. Chem*. 34 (2004) 1031.
42. B. Wang, H. Ma. *Synth. Reac. Inorg. Met. Org. Chem*. 34 (2004) 1009.
43. W. Wu, D.E. Vanderwall, S.M. Lui, X.J. Tang, C.J. Turner, J. W. Kozarich, J. Stubbe. *J. Am. Chem. Soc*. 118 (1996) 1268.
44. R.M. Issa, A.M. Khedr, H. Rizk, *J. Chin. Chem. Soc.* 55 (2008) 875.
45. M.E. Moustafa, E.H. El-Mossalamy, A.S. Amin. *Monatsh. Chem*. 126 (1995) 901.
46. H. Liu, H. Wang, F. Gao, D. Niu, Z. Lu. *J. Coord. Chem*. 60 (2007) 2671.
47. D.P. Singh, R. Kumar, V. Malik, P. Tyagi. *Trans. Met. Chem*. 32 (2007) 1051.
48. D. F. Shriver, P. W. Atkins, C. H. Langford. *Inorganic Chemistry*, Oxford University Press, Oxford (1990).
49. F.A. Cotton, G. Wilkinson, *Advanced Inorganic Chemistry*, 3rd Edit., Wiley, New York (1972).
50. B.J. Hathaway. *J. Struct. Bond*. 57 (1984) 55.
51. K.K. Narang, V.P. Singh. *Trans. Met. Chem*. 21 (1997) 507.
52. A. El-Dissouky, A.M. Hindaway, A. Abdel Salam. *Inorg. Chim. Acta* 118 (1986) 114.
53. I.M. Proctor, B.J. Hathaway, P. Nicholis. *J. Chem. Soc. A* (1972) 1229.
54. B.J. Hathaway, D.E. Billing. *Coord. Chem. Rev*. 5 (1970) 143.
55. M. Badea, A. Emandi, D. Marinescu, E. Cristurean, R. Olar, A. Braileanu, P. Budrugeac, E. Segal. *J. Therm. Anal. Calorim*. 72 (2003) 525.
56. F.A. Aly, S.M. Abu-El-Wafa, R.M. Issa, F.A. El-Sayed. *Thermochim. Acta* 126 (1988) 235.
57. D.L. Kallyman, J.P. Scorill, J.E. Batosevich, Bruce. *J. Med. Chem*. 26 (1983) 35.
58. K.N. Thimmaiah, W.D. Lloyd, G.T. Chandrappa. *Inorg. Chim. Acta.* 106 (1985) 81.
59. C.H. Collins, P. M. Lyne. *Microbiological Methods*, Butterworth, London (1976).
60. A. Kulkarni, P.G. Avaji, G.B. Bagihalli, P.S. Badami, S.A. Patil. *J. Coord. Chem*. 62 (2009) 481.
61. S. Malik, S. Ghosh, L. Mitu. *J. Serb. Chem. Soc.* 76 (2011) 1387.
62. Z.H. Chohan, H. Pervez, A. Rauf, C. T. Supuran. *Metal Based Drugs* 8 (2002) 263.
63. R. Olar, M. Badea, D. Marinescu, V. Lazar, C. Chifiriuc. *J. Therm. Anal. Calorim*. 97 (2009) 721.
64. M.A. El-Morsi, M. Gaber, R.M. Issa, M.M. Ghoneim. *J. Elecrochem. Soc.* 4 (1988) 956.